

NGL-15-003-002 Pub. of the  
Astronomical Society of the Pacific

Scanner Observations of Selected Cool Stars\*

Theodore D. Fay, Jr.

Department of Physics and Astronomy, University of Alabama

William L. Stein and Wayne H. Warren, Jr.

Department of Astronomy, Indiana University

Scanner Observations of Cool Stars

Send Proofs to: William L. Stein  
Wayne H. Warren, Jr.  
Swain Hall West 319  
Department of Astronomy  
Indiana University  
Bloomington, Indiana 47401

Theodore D. Fay, Jr.  
Box 1921  
Department of Physics and Astronomy  
University of Alabama  
University, Alabama 35486

Received:

27 March 1974

\*Publications of the Goethe Link Observatory, Indiana University, No. \_\_\_\_\_

(NASA-CR-138777) SCANNER OBSERVATIONS OF N74-27348  
SELECTED COOL STARS (Indiana Univ.)  
35 p HC \$4.75 CSCL 03A  
Unclas  
G3/30 41915

## ABSTRACT

Photoelectric spectral scans at 30-Å resolution of 9 dwarfs, 10 giants and 6 supergiants with spectral types G0 to M5 are presented. All stars were observed every 4 Å from  $\lambda 3300$  to  $\lambda 7000$ . Absorption features observed at this resolution coincide with strong atomic lines of Fe I, II, Ca I, II, Mg I, and Na I; vibrational bands of the electronic transitions of TiO, MgH, CaH, SiH, AlH, CN, CH, C<sub>2</sub>, OH, and NH. The dependence of the  $\lambda 3740$  Fe I blend and the  $\lambda 3440$  depression on temperature is discussed.

Key Words: spectrophotometry - cool stars - spectral line identification

PRECEDING PAGE BLANK NOT FILMED

## INTRODUCTION

Much of our information on the nature of cool stars depends upon a comparison of observed fluxes with those from model atmospheres. Previous spectrophotometry in the region 3300-7000 Å has been confined to studies of particular strong atomic and molecular features plus continuum points to determine temperature, gravity and abundance indicators (cf. van den Bergh and Sackman 1965; McClure and van den Bergh 1968; Spinrad and Taylor 1969). There are, however, no published continuous energy distributions of these stars from 3300 to 7000 Å available for detailed comparison with atmospheric models. The scanner observations presented here should be useful for this purpose since the relative fluxes are observed every 4 Å. It is also possible to use these scans to determine line blanketing, identify molecular features, or place narrow-band interference filters for measuring strong absorption features and continuum points in the energy distributions of similar stars.

Figures 1-6 display our scans of G0-M5 stars of different luminosities in the aforementioned wavelength range. Although the resolution is only about 30 Å, we oversample the data at 4-Å intervals both to allow more detailed comparison with models and to increase the accuracy of data reduction. Our resolution is sufficient to show strong atomic lines, molecular bands, and other continuum features. These scans should therefore indicate major sources of line opacity to be included in atmospheric models in this wavelength region.

## OBSERVATIONS

The observations were made during 1971 and 1972 at Goethe Link Observatory using equipment previously described by Honeycutt (1971). They were reduced to flux using a method described by Faÿ, Honeycutt and Warren (1973) and a detailed discussion of observational errors can be found there.

Table I lists the observed energy distributions of the program stars at Hayes (1970) standard wavelengths. All stars have been observed on more than one night, some on as many as five nights. The results presented are means which have been computed by weighting according to nightly errors. For known variables we present only the best individual observations and the corresponding dates are listed in the table. The solar scan shown for comparison in Figure 1 has a resolution of  $20 \text{ \AA}$  and is taken from Labs and Neckel (1968). In order to show the approximate extent of nightly variations for the bright stars, we display in Figures 3 and 6 two scans of  $\mu$  Cephei taken on different nights.

## DISCUSSION

## A. Strengths and Identifications of Atomic Line Features

We consider it worthwhile to identify the spectral features found at scanner resolution and to tabulate the strengths of these features.

Identification codes for the spectral features in Figures 1-6 are given in Tables II and III. Electronic transitions of molecular bands are indicated by small Greek symbols and strong atomic lines by small Roman symbols.

Many of the atomic line identifications in Table II are Fe I lines of solar equivalent width greater than  $1 \text{ \AA}$  (Moore et al. 1966). Each spectral feature at  $30\text{-}\text{\AA}$  resolution is composed of from 2-10 blended lines. Our atomic line codes are given in column 2 of the first part of Table II while the wavelengths of the lines contributing to each blend are listed in column 3. Solar equivalent widths and lower excitation potentials are given in columns 4 and 5 and are taken from Moore et al. (1966). Column 6 lists the solar identifications of the atomic line blends; there are 43 line blends of H, Fe I, Mg I, Ca I, Ca II, Mn I and Na I included in the table.

In Table IV we tabulate the strengths of some of the line blends identified in Tables II and III. Column 2 lists the wavelengths of the blends and continuum points; the remaining columns tabulate the strengths of line blends in each of the program stars in flux differences measured in magnitudes. An example of the temperature dependence of the Fe I strengths from Table IV is shown in Figure 7. The peak strength of this blend (1f,  $\lambda 3740$ ) occurs at spectral type K5. The decrease in strength of the  $\lambda 3740$  feature for spectral types later than K5 must be due to some source of opacity which absorbs more at the reference wavelength ( $\lambda 3680$ ) than at  $\lambda 3740$ . Line blanketing by OH and CH is a possible source for this absorption.

Tarafdar and Vardya (1972) show that line blanketing by CH and OH is the strongest opacity source between 3000-4000 Å at temperatures cooler than 5000 K. Vardya (1966) and Greene (1972) have computed partial pressures for OH and CH. For solar abundances, Greene's results show that the partial pressure of OH increases by a factor greater than 1000 as  $\theta$  varies from 1.0 to 2.2 while the partial pressure of CH decreases by more than  $10^6$ . The computations of Tarafdar and Vardya demonstrate that OH line blanketing decreases sharply between 3500-3800 Å. Therefore we would expect that OH should absorb more at the reference wavelength than at  $\lambda 3740$ .

#### B. Identifications of Molecular Bands

Table III lists the identifications of molecular line blends seen on our scans. The second part of the table defines the molecular codes used in the first part and in the figures. Each electronic transition is given a different Greek letter and/or Arabic number. The first part of the table lists the title of each electronic transition in column 1, the molecular identification code assigned in column 2 and the vibrational band and wavelength of the blend in columns 3 and 4.

Pearse and Gaydon (1963) was used as a general reference for the wavelengths of each molecule considered in Table III. We used the following references to identify the strong TiO features: Gattareri, Junkes, Salpeter and Rosen (1957), Phillips (1969, 1971), Phillips and Davis (1971), Wentink and Spindler (1972). The MgH depressions (Moore et al. 1966) are very strong on our spectra, as can be seen in Figures 1-6. Spinrad and Taylor (1969) have made scanner studies of the strengths of these and the TiO bands in this spectral region. Webber (1971) has identified and studied CaH lines at high resolution in sunspot spectra from  $\lambda 6200$ - $\lambda 6400$ . Vardya (1966) indicates that ratios of partial pressures of MgH/CaH are equal to 20 at  $\tau = 2/3$  for M4 V. Spinrad and Taylor (1969) have made the most recent scanner studies of the

stellar CaH depression at  $\lambda 6350$ . As seen in Figures 3-6, our observations are consistent with earlier work.

Sauval (1969) has identified the SiH (0,0) band at  $\lambda 4140$  in sunspot spectra. In the spectrum of  $\beta$  Peg, Davis (1947) finds that next to TiO and MgH, SiH produces the strongest molecular absorption. On our stellar scans in Figures 1-3, these and other SiH bands have been identified. As expected these depressions are weak, since Vardya (1966) gives the partial pressure ratio of MgH/SiH = 30 at  $\tau = 2/3$  for M2 V.

Sotirovski (1972) claims to have identified AlH lines from 5000-7000  $\text{\AA}$  on high resolution sunspot spectra. However Wöhl (1971) has questioned these identifications. According to Davis (1947), the (0,0) transition of AlH at  $\lambda 4241$  is one of the strongest molecular absorption features in  $\beta$  Peg while other transitions are far less conspicuous. Computations by Vardya (1966) indicate that the ratio of partial pressures of MgH to AlH in M2 V stars is about 10 at  $\tau = 2/3$ . As predicted, features coincident with AlH are at least a factor of three weaker than the MgH features on Figures 1 and 4.

The identifications of the  $4\gamma$  features have been suggested by Pesch (1972) as due to CaOH. These features are strong only in Barnard's star (BD + 4° 3561, M5 V). Triatomic molecular formation would be likely only at the highest pressures and/or lowest temperatures found in stellar atmospheres.

We now briefly review the known molecular compounds of H, C, N and O which are strong in stellar spectra: CH, OH, NH, CN and  $C_2$ . Table III indicates the wavelengths of the stronger bands of these light molecules, and some of their strengths measured from our scans are given in Table IV.

Lambert and Beer (1972) have observed strong OH absorption features in  $\alpha$  Orionis near 3 microns. These vibration-rotation bands of OH have  $f$  values which are a factor of 100 smaller than the electronic system. Tarafdar and Vardya (1972) have determined that OH is an important opacity source for cool stars in the wavelength range 3000-4000  $\text{\AA}$ . The bands of the  $\Delta v = -1$  sequence

of the OH molecule degrade longward of  $\lambda 3400$ . The minimum flux in the  $\lambda 3400$  depression seems to occur on our scans near  $\lambda 3440$  for dwarfs.

We have chosen  $\lambda 3540$  as a reference wavelength to measure the  $\lambda 3440$  depression because the highest flux levels between 3300-3600 Å occur at  $\lambda 3540$ . A referee has pointed out that the  $\lambda 3540$  reference wavelength is contaminated by the  $\Delta v = +1$  sequence of CN beginning at  $\lambda 3590$ . Because of this CN contamination, we have confined our analysis to the dwarf stars. For this luminosity class, the  $\lambda 3590$  band is weakest and the dependence of CN absorption upon temperature is minimal as shown by Wing (1967). The range of OH depression strengths shown in Figure 8 exceeds the range in CN strengths given by Wing for the dwarfs. The OH strength is defined by the  $[0.344] - [0.354] - \mu$  color which is expressed by  $-2.5 \log [F_{\nu}(3440)/F_{\nu}(3540)]$ . The solid line is the relative partial pressure ratio,  $P_{OH}/P_g$ , for  $\tau = 2/3$  as calculated by Vardya (1966). This OH feature is probably blended with atomic lines given in Table II if the  $[0.344] - [0.354] - \mu$  color is less than 0.2 magnitudes.

### C. Notes on Individual Stars

#### Binaries

The system  $\zeta$  Aur is a well known eclipsing binary (see e.g. Wilson 1960). We observed this variable on January 1, 1972 during total eclipse so that only the spectrum of the K4 Ib star is visible. The K4 primary's spectral energy distribution appears normal for its spectral and luminosity class as can be seen from the scans shown in Figures 3 and 6. The  $\alpha$  Her AB system is a visual pair. For this system we made an attempt to exclude the secondary from the entrance slot of the scanner by offsetting  $\alpha$  Her A from the center of the slot. Since the secondary is a single line spectroscopic binary of type G0 II-III (Deutsch 1960), some contamination of the spectrum is probable



shortward of  $4000 \text{ \AA}$ , but the value at each wavelength is difficult to estimate.

The  $\alpha$  Sco AB visual system has a separation of only  $3''$  and no attempt was made to exclude the B4 V companion from the entrance slot. Spectral classification of the B4 companion was made by Stone and Struve (1954); the visual magnitude difference of primary and secondary ( $\Delta m_{\text{vis}} = 4.25$ ) is from Wierzbinski (1969). If we compare the observed energy distribution of  $\alpha$  Ori shown in Figure 3 to the energy distributions of the B stars studied by Faÿ et al. (1973) with the same scanner, we note that an M and B star which differ by 4.2 mag at  $5500 \text{ \AA}$  would differ by less than 0.5 mag at  $3800 \text{ \AA}$ . The weakening of the spectral line features in  $\alpha$  Sco at wavelengths shortward of  $4000 \text{ \AA}$  is consistent with the observed visual magnitude differences and derived energy distributions for normal M2 I and B4 V stars.

## SUMMARY

Line blanketing features observed at 30-Å resolution for normal stars of spectral classes G0 to M5 can be identified with known atomic or molecular line blends observed in sunspot and stellar spectra of higher resolution. We conclude that many of the atomic line strengths (especially for types later than middle K) are strongly affected at scanner resolution by molecular line blanketing from the electronic transitions of TiO, MgH, CN, CH, OH, C<sub>2</sub>, NH, CaH, AlH, and SiH. Observed strengths of the λ3440-OH feature vary approximately with spectral class as do the partial OH pressures computed by Vardya (1966).

**ACKNOWLEDGEMENTS**

This work was supported by NASA Grant 15-003-002 to Hollis R. Johnson. The authors acknowledge helpful comments and encouragement from R. Kent Honeycutt, R. F. Wing and G. W. Lockwood. We also wish to thank an anonymous referee for his thoroughness and constructive criticism.

## FIGURE CAPTIONS

- Figure 1. Scans of G, K and M dwarfs in the range  $\lambda\lambda 3300-5300$ . Resolution is about  $30 \text{ \AA}$  and data spacing is  $4 \text{ \AA}$ . Identification codes are listed in Tables II and III.
- Figure 2. Same as Figure 1 for G, K and M giants.
- Figure 3. Same as Figure 1 for G, K and M supergiants.
- Figure 4. Scans of G, K and M dwarfs in the range  $\lambda\lambda 5000-7000$ . Other comments same as Figure 1.
- Figure 5. Same as Figure 4 for G, K and M giants.
- Figure 6. Same as Figure 4 for G, K and M supergiants.
- Figure 7. Strength of the Fe I depression (in mag) against spectral type. Filled circles are dwarfs, open circles giants, and open triangles supergiants.
- Figure 8. Dependence of the OH band depression ( $\lambda 3440$ ) on temperature for dwarf stars only. The solid line represents calculations by Vardya.

## REFERENCES

- Bergh, S. van dan, and Sackmann, I. J. 1965, A.J. 70, 353.
- Davis, D. N. 1947, Ap.J. 106, 28.
- Deutsch, A. J. 1960, in Stellar Atmospheres, J. Greenstein, ed. (Chicago: University of Chicago Press), p. 543.
- Fay, T., Honeycutt, R. K. and Warren, W. H. Jr. 1973, A.J. 78, 246.
- Getterer, A., Junkes, J., Salpeter, E. W. and Rosen, B. 1957, Molecular Spectra of Metallic Oxides (Vatican City: Vatican Observatory).
- Greene, A. E. 1972, Contr. Perkins Obs. Ser. 11, No. 31.
- Hayes, D. S. 1970, Ap.J. 159, 165.
- Honeycutt, R. K. 1971, Applied Optics 10, 1125.
- Labs, D. and Neckel, H. 1968, Zs. f. Ap. 69, 1.
- Lambert, D. L. and Beer, R. 1972, Ap.J. 177, 541.
- McClure, R. D. and Bergh, S. van den 1968, A.J. 73, 313.
- Moore, C. E., Minnaert, M. G. J. and Houtgast, J. 1966, National Bureau of Standards Monograph 61.
- Pearse, R. W. B. and Gaydon, A. G. 1963, The Identification of Molecular Spectra (New York: John Wiley and Sons).
- Pesch, P. 1972, Ap.J. (Letters) 174, L155.
- Phillips, J. G. 1969, Ap.J. 157, 449.
- \_\_\_\_\_. 1971, Ap.J. 169, 185.
- Phillips, J. G. and Davis, S. P. 1971, Ap.J. 167, 209.
- Sauval, A. J. 1969, Solar Physics 10, 319.
- Sotirovski, P. 1972, Astr. and Ap. Suppl. 6, 85.
- Spinrad, H. and Taylor, B. J. 1969, Ap.J. 157, 1279.
- Stone, S. N. and Struve, O. 1954 Pub.A.S.P. 66, 191.

- Tarafdar, S. P. and Vardya, M. S. 1972, Ap.J. 171, 185.
- Vardya, M. S. 1966, M.N.R.A.S. 134, 347.
- Webber, J. C. 1971 Solar Physics 16, 340.
- Wentink, T. Jr. and Spindler, R. J. Jr. 1972, Journ. Quant. Spectrosc.  
Radiat. Transfer 12, 1569.
- Wierzbinski, S. 1969, Contr. Wroclaw Astr. Obs. No. 16.
- Wilson, O. C. 1960, in Stellar Atmospheres, J. Greenstein, ed. (Chicago:  
University of Chicago Press), p. 436.
- Wing, R. F. 1967, Doctoral Dissertation, University of California, Berkeley.
- Wohl, H. 1971, Solar Physics 16, 362.

TABLE I

Relative Magnitudes at Hayes Points Normalized at 5263 Å

Stars*	3400Å	3450Å	3500Å	3571Å	3636Å	3705Å	3862Å	4037Å	4168Å
$\beta$ Com	1. <sup>m</sup> 506	1. <sup>m</sup> 568	1. <sup>m</sup> 440	1. <sup>m</sup> 410	1. <sup>m</sup> 258	1. <sup>m</sup> 150	1. <sup>m</sup> 078	0. <sup>m</sup> 431	0. <sup>m</sup> 433
$\tau$ Cet			1.695	1.775	1.476	1.429	1.547	0.777	0.642
$\epsilon$ Eri			2.000	2.270	1.715	1.810	2.110	1.020	0.843
61 Cyg A			2.811	3.027	2.754	2.621	2.857	1.660	1.337
61 Cyg B			3.114	3.212	2.966	2.851	2.983	1.931	1.511
GRM 1618					2.895	2.821	2.657	1.879	1.539
LA 21185								1.815	1.621
+15° 2620								1.870	1.626
+4° 3561									
31 Com	1.797	1.779	1.710	1.681	1.599	1.336	1.225	0.665	0.563
$\epsilon$ Vir	2.174	2.205	2.090	2.306	1.792	1.665	2.268	0.950	1.043
$\alpha$ UMa	2.647	2.758	2.579	2.785	2.255	2.119	2.421	1.187	1.238
$\alpha$ Boo	3.171	3.206	3.004	3.258	2.691	2.568	2.931	1.506	1.445
$\alpha$ Hya			3.915	3.990	3.523	3.429	3.779	2.152	2.065
$\alpha$ Tau			3.730	3.938	3.502	3.451	3.594	2.238	1.968
$\alpha$ Cet			4.071	4.266	3.796	3.587	3.571	2.379	2.081
$\delta$ Vir			4.151	4.129	3.709	3.610	3.480	2.303	1.905
$\omega$ Vir			3.982	4.036	3.515	3.461	3.317	2.163	1.717
$\alpha$ Her A (6/23/71)					3.195	3.068	2.926	1.759	1.402
$\epsilon$ Gem			3.574	3.670	2.923	2.882	3.243	1.880	1.938
$\zeta$ Aur (1/1/72)				4.080	3.552	3.390	3.615	2.320	2.165
$\sigma$ CMA							3.598	2.385	2.181
$\alpha$ Sco AB				4.088	3.898	3.753	3.495	2.608	2.317
$\alpha$ Ori (2/5/72)					3.996	3.903	3.648	2.594	2.245
$\mu$ Cep (10/31/71)							4.056	3.373	2.809

\*Date indicated if star is variable.

TABLE I (continued)

4255Å	4464Å	4566Å	4787Å	5000Å	5263Å	5559Å	5841Å	6057Å	6439Å	6793Å
0. <sup>m</sup> 422	0. <sup>m</sup> 243	0. <sup>m</sup> 165	0. <sup>m</sup> 066	0. <sup>m</sup> 047	0. <sup>m</sup> 000	-0. <sup>m</sup> 149	-0. <sup>m</sup> 187	-0. <sup>m</sup> 220	-0. <sup>m</sup> 260	-0. <sup>m</sup> 308
0.676	0.334	0.229	0.107	0.065	0.000	-0.170	-0.243	-0.292	-0.378	-0.453
0.829	0.357	0.155	0.034	0.079	0.000	-0.203	-0.369	-0.427	-0.527	-0.669
1.433	0.685	0.364	0.340	0.215	0.000	-0.190	-0.279	-0.338	-0.463	-0.553
1.595	0.781	0.425	0.461	0.296	0.000	-0.495	-0.741	-0.817	-0.985	-1.055
1.602	0.781	0.422	0.461	0.345	0.000	-0.514	-0.728	-0.794	-1.038	-1.074
1.796	0.894	0.579	0.482	0.479	0.000	-0.337	-0.523	-0.604	-0.884	-0.711
1.855	0.820	0.620	0.561	0.429	0.000	-0.605	-1.005	-1.175	-1.621	-1.590
2.993	1.718	1.198	1.402	0.715	0.000	-0.083	-0.651	-0.700	-1.314	-1.148
0.518	0.344	0.254	0.102	0.070	0.000	-0.194	-0.263	-0.300	-0.341	-0.398
0.782	0.450	0.336	0.126	0.103	0.000	-0.232	-0.368	-0.425	-0.530	-0.651
0.920	0.552	0.386	0.137	0.080	0.000	-0.304	-0.451	-0.518	-0.595	-0.691
1.229	0.707	0.493	0.241	0.169	0.000	-0.363	-0.562	-0.676	-0.788	-0.929
1.690	0.945	0.658	0.290	0.133	0.000	-0.448	-0.675	-0.818	-0.954	-1.130
1.716	0.945	0.611	0.431	0.272	0.000	-0.474	-0.717	-0.882	-1.082	-1.193
1.895	1.095	0.735	0.540	0.349	0.000	-0.497	-0.769	-0.985	-1.282	-1.358
1.789	1.048	0.700	0.671	0.528	0.000	-0.362	-0.487	-0.739	-1.141	-1.057
1.670	1.170	0.823	0.898	0.770	0.000	-0.259	-0.349	-0.678	-1.239	-1.138
1.419	1.296	0.858	0.984	0.889	0.000	-0.443	-0.638	-0.968	-1.564	-1.552
1.411	0.938	0.673	0.191	0.146	0.000	-0.429	-0.622	-0.703	-0.727	-0.865
1.804	1.065	0.747	0.366	0.178	0.000	-0.600	-0.885	-1.052	-1.219	-1.453
1.787	1.150	0.715	0.318	0.181	0.000	-0.524	-0.755	-0.974	-1.210	-1.402
2.074	1.471	1.059	0.611	0.396	0.000	-0.543	-0.813	-1.023	-1.388	-1.534
2.008	1.394	0.952	0.556	0.376	0.000	-0.589	-0.843	-1.127	-1.443	-1.524
2.602	1.960	1.457	0.902	0.554	0.000	-0.581	-0.970	-1.267	-1.624	-1.802



TABLE II  
Atomic Line Blends at 30 Å Resolution

Blend No.	Atomic Code	Wave-length Å	Solar Weq Å	Low EP eV	Solar Ident.	Blend No.	Atomic Code	Wave-length Å	Solar Weq Å	Low EP eV	Solar Ident.		
1	7a	3361.2	0.9	0.9	TiI, TiII	12	1g	3797.9	3.5	10.2	H 10		
2	6a	3380.9	0.8	0.4	Ni I		or	3795.0	0.5	1.0	Fe I		
		3384.0	0.4	3.0	Fe I		2g	3799.6	0.6	1.0	Fe I		
		3394.0	0.6	0.0	Ni I			3815.9	1.3	1.5	Fe I		
3	6b	3414.8	0.8	0.0	Ni I			3820.4	1.7	0.9	Fe I		
		3433.6	0.5	0.0	Ni I			3825.9	1.5	0.9	Fe I		
		3446.2	0.5	0.1	Ni I			3824.4	0.5	0.0	Fe I		
		1a	3440.6	1.2	0.0		Fe I	3a	3827.8	0.9	1.6	Fe I	
										3834.2	0.6	1.0	Fe I
4	6c	3458.5	0.7	0.2	Ni I		3829.3	0.9	2.7	Mg I			
		3461.7	0.8	0.0	Ni I		3832.0	1.7	2.7	Mg I			
		3465.9	0.5	0.1	Fe I		3838.3	1.9	2.7	Mg I			
5	1b	3475.4	0.6	0.1	Fe I	13	lh	3856.4	0.7	0.0	Fe I		
		3476.7	0.5	0.1	Fe I		or	3859.9	1.6	0.0	Fe I		
		3490.6	0.8	0.0	Fe I		2h	3872.5	0.6	1.0	Fe I		
		3497.8	0.7	0.1	Fe I			3878.0	0.6	1.0	Fe I		
		6d	3493.0	0.8	0.1		Ni I		3878.6	0.7	0.0	Fe I	
6	6e	3510.3	0.5	0.2	Ni I		3886.3	0.9	0.0	Fe I			
		3515.1	0.7	0.1	Ni I		3889.0	2.3	10.2	H 8			
		3524.5	1.3	0.0	Ni I	14	8a	3905.5	0.9	1.9	Si I		
7	1c	3565.4	1.0	1.0	Fe I	15	4a	3933.7	20	0.0	Ca II K		
		3570.1	1.4	0.9	Fe I		4b	3968.5	15	0.0	Ca II H		
		3581.2	2.1	0.9	Fe I		16	1i	4045.8	1.2	1.5	Fe I	
		3585.3	0.8	1.0	Fe I				4063.6	0.8	1.6	Fe I	
		3587.0	0.5	1.0	Fe I				4071.7	0.7	1.6	Fe I	
8	1d	3608.9	1.0	1.0	Fe I	17	2d	4101.7	3.1	10.2	H 8		
		3618.8	1.4	1.0	Fe I		18	1j	4132.0	0.4	1.6	Fe I	
		3631.5	1.4	1.0	Fe I				4143.9	0.5	1.6	Fe I	
		3647.9	1.0	0.9	Fe I			19	5a	4226.7	1.5	0.0	Ca I
9	1e	3679.6	0.5	0.0	Fe I	20	G		4250.8	0.4	1.6	Fe I	
		3687.5	0.6	0.0	Fe I				4260.5	0.6	2.4	Fe I	
		3705.6	0.6	0.0	Fe I			4271.8	0.8	1.5	Fe I		
10	2e	3646.0			Balmer Limit								
11	1f or 2f	3721.9	0.5	10.2	H 14			4254.3	0.4	0.0	Cr I		
		3719.9	1.6	0.0	Fe I			4271.1	0.2	3.1	Cr I		
		3722.6	0.7	0.0	TiI + FeI			4274.8	0.2	0.0	Cr I		
		3727.6	0.6	1.0	Fe I			4283.0	0.1	1.9	Ca I		
		3734.4	1.0	10.2	H 13			4302.5	0.2	1.9	Ca I		
		3734.9	3.0	0.9	Fe I			4307.9	0.7	1.6	Fe I		
		3737.1	1.1	0.0	Fe I			4325.8	0.8	1.6	Fe I		
		3743.4	0.6	1.0	Fe I	21	2c	4340.5	2.9	10.2	H γ		
		3745.6	1.2	0.1	Fe I			22	1k	4383.6	1.0	1.5	Fe I
		3749.5	1.9	0.9	Fe I						4404.8	0.9	1.6
		3750.1	1.4	10.2	H 12			4415.0	0.4	1.6	Fe I		
		3758.2	1.6	1.0	Fe I								
		3763.8	0.8	1.0	Fe I								
		3767.2	0.8	1.0	Fe I								
		3770.6	1.9	10.2	H 11								

TABLE II (continued)

Blend No.	Atomic Code	Wave-length Å	Solar Weq Å	Low EP eV	Solar Ident.	Blend No.	Atomic Code	Wave-length Å	Solar Weq Å	Low EP eV	Solar Ident.		
23	5b	4423.3	0.1	2.1	Na I	32	lq	4978.6	0.1	4.0	Fe I		
		4425.4	0.1	1.9	Ca I			4980.2	0.1	3.6	Ni I		
		4427.3	0.1	0.0	Fe I			4981.7	0.1	0.9	Ti I		
		4435.0	0.2	1.9	Ca I			4982.5	0.1	4.1	Fe I		
		4435.7	0.1	1.9	Ca I			4983.2	0.1	4.2	Fe I		
		4444.5	0.4	2.0	Fe I			4983.8	0.1	4.1	Fe I		
		4454.8	0.2	1.9	Ca I			4985.2	0.1	3.9	Fe I		
24	ll	4522.5	0.1	2.8	Fe II			4985.5	0.1	2.9	Fe I		
		4525.1	0.1	3.6	Fe I			4991.0	0.1	0.8	Ti I		
		4526.4	0.1	3.9	Fe I			4994.1	0.1	0.9	Fe I		
		4528.6	0.3	2.2	Fe I			4999.5	0.1	0.8	Ti I		
		4529.5	0.1	1.6	Ti II			5001.9	0.2	3.9	Fe I		
		4531.2	0.1	1.5	Fe I			5005.7	0.1	3.9	Fe I		
		4534.0	0.1	1.2	Ti II			5006.1	0.2	2.8	Fe I		
		4549.5	0.2	2.0	FeII+TiIII	5007.3	0.2	0.8	Ti I				
25	5c	4581.4	0.2	2.5	CaI + FeI	5012.0	0.2	0.8	Fe I				
		4585.9	0.1	2.5	Ca I	5014.2	0.2	0.0	Ti I				
		4578.6	0.1	2.5	Ca I	5015.0	0.1	3.9	Fe I				
		4583.9	0.1	3.1	FeI + Fe II	5018.4	0.2	2.9	Fe II				
		26	lm	4637.5	0.1	3.2	Fe I	33	lr	5035.4	0.1	3.6	Ni I
4654.6	0.2			2.0	Fe I	5035.9	0.1			1.5	Ti I		
4668.1	0.1			3.4	Fe I	5040.9	0.1			4.3	Fe I		
27	3a			4703.0	0.3	4.3	Mg I			5041.0	0.1	1.0	Fe I
				4707.3	0.1	3.2	Fe I			5041.8	0.2	1.5	Fe I
				4709.0	0.1	2.0	Ti I			5049.8	0.1	2.2	Fe I
				4710.3	0.1	3.0	Fe I			5051.6	0.1	0.9	Fe I
				4714.4	0.1	3.4	Ni I			5065.0	0.1	4.3	Fe I
				4727.4	0.1	3.6	Fe + Mn			5068.8	0.1	2.9	Fe I
				4736.8	0.1	3.2	Fe			5074.7	0.1	4.2	Fe I
		28	9a	4754.0	0.1	2.0	Mn I	34	3b	5167.3	1.0	2.7	MgI + FeI
4762.4	0.1			2.9	Mn I	5172.7	1.3			2.7	Mg I		
4768.4	0.1			3.7	Fe I	5183.6	1.6			2.7	Mg I		
4783.4	0.2			2.3	Mn I	35	ls			5188.7	0.2	1.6	TiII+CaI
4786.5	0.1			3.4	Ni I					5191.5	0.2	3.0	Fe I
29	2b ln	4861.3	3.7	10.2	H β			5192.4	0.2	3.0	Fe I		
		4871.3	0.2	2.9	Fe I			5193.0	0.1	0.0	Ti I		
		4872.1	0.2	2.9	Fe I			5194.9	0.2	1.6	Fe I		
		4878.2	0.2	2.9	CaI + Fe I			5202.3	0.2	2.2	Fe I		
		4890.8	0.2	2.9	Fe I			5204.5	0.2	0.9	CrI+FeI		
		4891.5	0.3	2.9	Fe I			5206.0	0.2	0.9	Cr I		
		30	lo	4919.0	0.3			2.9	Fe I	5208.4	0.2	0.9	Cr I
				4920.5	0.5			2.9	Fe I	36	lt or 5d	5227.2	0.3
4923.9	0.2			2.9	Fe II	5233.0	0.3	2.9	Fe I				
4924.8	0.1			2.2	Fe I	5264.0	0.2	2.5	Ca I				
31	lp			4957.6	0.7	2.8	Fe I	5265.6	0.1			2.5	Ca I
		5266.5	0.3	0.8	Ti I	5269.5	0.5	0.9	Fe I				
		5270.3	0.3	1.6	CaI + FeI	5270.3	0.3	1.6	CaI + FeI				
		5273.2	0.1	3.3	Fe I	5273.2	0.1	3.3	Fe I				
		5273.4	0.1	2.5	Fe I	5273.4	0.1	2.5	Fe I				
		5276.1	0.1	2.9	Cr I	5276.1	0.1	2.9	Cr I				
		5281.7	0.2	3.0	Fe I	5281.7	0.2	3.0	Fe I				
		5283.6	0.2	3.2	Fe I	5283.6	0.2	3.2	Fe I				

TABLE II (continued)

Blend No.	Atomic Code	Wave-length Å	Solar Weq Å	Low EP eV	Solar Ident.	Blend No.	Atomic Code	Wave-length Å	Solar Weq Å	Low EP eV	Solar Ident.		
37	lu	5324.0	0.3	3.2	Fe I	39	5e	5582.0	0.1	2.5	Ca I		
		5328.0	0.4	0.9	Fe I			5588.8	0.1	2.5	Ca I		
		5328.5	0.2	1.6	Fe I			5590.1	0.1	2.5	Ca I		
		5332.9	0.1	1.6	Fe I			5594.5	0.1	2.5	Ca I		
		5339.9	0.2	3.2	Fe I			5598.4	0.1	2.5	Ca I		
		5341.1	0.2	1.6	Fe I			5601.3	0.1	2.5	Ca I		
38	lv	5371.5	0.3	1.0	Fe I			5602.9	0.1	2.5	Ca I		
		5384.4	0.2	4.3	Fe I			5615.6	0.3	2.5	Ca I		
		5393.2	0.2	3.2	Fe I			40	D	5890.0	0.8	0.0	Na I
		5397.1	0.2	0.9	Fe I					5896.0	0.6	0.0	Na I
		5400.5	0.1	4.4	Fe I			41	5f	6102.7	0.1	1.9	Ca I
		5404.1	0.2	4.3	Fe I					6122.2	0.2	1.9	Ca I
		5405.8	0.3	1.0	Fe I	6136.6	0.1			2.4	Fe I		
		5415.2	0.2	4.4	Fe I	6137.7	0.1			2.6	Fe I		
		5424.0	0.2	4.3	Fe I	6141.7	0.1			3.6	Fe I		
		5429.8	0.3	1.0	Fe I	6162.2	0.2			1.9	Ca I		
		5434.5	0.2	1.0	Fe I	6169.5	0.1			2.5	Ca I		
		5446.9	0.2	1.0	Fe I	42	5g			6439.0	0.2	2.5	Ca I
		5455.6	0.2	1.0	Fe I			6462.6	0.2	2.5	CaI + FeI		
								43	2a	6562.8	4.0	10.2	H α

Atomic Line Code Identification

Code	Atom
1	Fe I
2	H (Balmer)
3	Mg I
4	Ca II
5	Ca I
6	Ni I
7	Ti I
8	Si I
9	Mn I

TABLE III  
MOLECULAR BANDS AT 30-Å RESOLUTION

ELECTRONIC SYSTEM	MOLECULAR CODE	VIBRATION BAND	WAVELENGTH Å	ELECTRONIC SYSTEM	MOLECULAR CODE	VIBRATION BAND	WAVELENGTH Å	
$C^3\Delta-X^3\Delta$ (T10)	$1\alpha_3$	3,0	4584	$B^3\Pi-X^3\Delta$ (T10)	$1\gamma_2$	1,0 R <sub>3</sub>	6651	
		4,1	4626			1,0 R <sub>2</sub>	6680	
		5,2	4668			1,0 R <sub>1</sub>	6713	
	$1\alpha_2$	2,0	4761			2,1 R <sub>3</sub>	6746	
		3,1	4804			3,2 R <sub>3</sub>	6814	
		4,2	4848			4,3 R <sub>3</sub>	6852	
	$1\alpha_1$	1,0	4954			$1\gamma_0$	0,0 R <sub>3</sub>	7053
		2,1	4999				0,0 R <sub>2</sub>	7087
	$1\alpha_0$	0,0	5167				0,0 R <sub>1</sub>	7124
		?	5307				1,1 R <sub>1</sub>	7197
		?	5356			2,2 R <sub>3</sub>	7270	
	$1\alpha_{-1}$	0,1	5448			$1\gamma_1^1$	1,0 R <sub>1</sub>	5847
		1,2	5497				2,1 R <sub>3</sub>	5951
	$1\alpha_{-2}$	0,2	5760				3,2 R <sub>3</sub>	6003
		1,3	5810				4,3 R <sub>3</sub>	6058
$a^1\Delta-C^1\Phi$ (T10)	$1\beta_0$	0,0	5600	$1\gamma_0^1$	0,0 R <sub>1</sub>	6158		
		1,1	5631		0,0 R <sub>2</sub>	6186		
		2,2	5663		0,0 R <sub>3</sub>	6214		
		3,3	5697		1,1 R <sub>2</sub>	6240		
		4,4	5727		1,1 R <sub>3</sub>	6276		
$A^3\Phi-X^3\Delta$ (T10)	$1\gamma_2$	2,0 R <sub>2</sub>	6322	$1\gamma_{-1}^1$	0,1 R <sub>1</sub>	6569		
		3,1 R <sub>3</sub>	6358		0,1 R <sub>2</sub>	6596		
		4,2 R <sub>2</sub>	6448		0,1 R <sub>3</sub>	6629		
		5,3 R <sub>1</sub>	6512		1,2 R <sub>2</sub>	6649		
				$e^1\Sigma-d^1\Sigma$ (T10)	$1\epsilon_0$	0,0	4114	

TABLE III (continued)

ELECTRONIC SYSTEM	MOLECULAR CODE	VIBRATION BAND	WAVELENGTH Å	ELECTRONIC SYSTEM	MOLECULAR CODE	VIBRATION BAND	WAVELENGTH Å		
$D^3\Pi-X^3\Delta$ (TiO)	1 $\eta$	0,0	3286-	$3\alpha_{-2}$	0,2 R	4886	3650		
							0,2 Q	4929	
							1,3	5031	
$A^2\Pi-X^2\Sigma$ (MgH)	2 $\alpha_1$	1,0	4845	$3\alpha_{-3}$	0,3	5314			
							5211	1,4	5430
							5186		
							5182		
	2 $\alpha_0$	0,0 R	5155	$3\beta_0$	0,0	4723			
			0,0 Q						
	2 $\alpha_{-1}$	0,1	5621	$E^1\Pi-A^1\Pi$ (AlH)	3 $\gamma_0$	0,0	3382		
			1,2						
			2,3						
	2 $\alpha_{-2}$	0,2	6083	$b^3\Pi-a^3\Pi$ (AlH)	3 $\delta_0$	0,0	3810		
$A^2\Pi-X^2\Sigma$ (CaH)	2 $\beta_0$	0,0 Q <sub>2</sub>	6920	$A^2\Delta-X^2\Delta$ (SiH)	3 $\epsilon_1$	3870			
		0,0 P <sub>2</sub>	7035						
$B^2\Sigma-X^2\Sigma$ (CaH)	2 $\beta_{-1}$	0,1	7567		3 $\epsilon_0$	4128			
							6346	0,0 Q <sub>1</sub>	4142
								0,0 Q <sub>2</sub>	4190
$A^1\Pi-X^1\Sigma$ (AlH)	3 $\alpha_1$	1,0	4066	$(CaOH)$	4 $\gamma$	5550			
							4241	5730	
							4357		
	3 $\alpha_0$	0,0	4450		5 $\alpha_0$	0,0	4320		
			1,1					6230	
		2,2	4450		5 $\alpha_{-1}$	0,1	4890		
	3 $\alpha_{-1}$	0,1 R	4546	$A^2\Delta-X^2\Pi$ (CH)					
0,1Q			4576						

TABLE III (continued)

ELECTRONIC SYSTEM	MOLECULAR CODE	VIBRATION BAND	WAVELENGTH Å	ELECTRONIC SYSTEM	MOLECULAR CODE	VIBRATION BAND	WAVELENGTH Å
$B^2\Sigma-X^2\Pi$ (CH)	$5B_0$	0,0	3880	$A^2\Pi_g-X'^3\Pi_u$ (C <sub>2</sub> SWAN)	$7\alpha$	0,0	5165
		1,1	4030			0,1	5635
	$5B_{-1}$	1,2	4496		$8\alpha_0$	1,1 Q	3370
$A^2\Pi-X^2\Sigma$ (CN)	$6\alpha_7$	8,1	4832			0,0 Q	3360
		9,2	4936			0,0 R	3302
		10,3	5043				
	$6\alpha_8$	6,0	5129				
		7,1	5239				
		8,2	5354				
		9,3	5473				
		10,4	5598				
	$6\alpha_9$	5,0	5606				
		6,1	5730				
		7,2	5858				
		8,3	5993				
9,4		6132					
$6\alpha_4$	4,0	6192					
	5,1	6332					
	6,2	6478					
	7,3	6631					
	8,4	6791					
$B^2\Sigma-X^2\Sigma$ (CN)	$6B_3$	1,0	3590				
	$6B_0$	0,0	3883				
	$6B_{-1}$	0,1	4216				
	$6B_{-2}$	0,2	4606				
		1,3	4578				
				$A^2\Sigma^+-X^2\Pi$ (OH)	$9\alpha_{-1}$	0,1 R	3430
						0,1 Q	3465
					$9\alpha_{-2}$	0,2 R	3890
						0,2 Q	3933
					$9\alpha_{-3}$	0,3 R	4450
						0,3 Q	4506

TABLE III (continued)

## MOLECULAR CODE IDENTIFICATION

CODE	MOLECULE	CODE	MOLECULE
1 $\alpha$ - $\eta$	TiO	5 $\alpha$ , $\beta$	CH
2 $\alpha$	MgH	6 $\alpha$ , $\beta$	CN
2 $\beta$ , $\gamma$	CaH	7 $\alpha$	C <sub>2</sub> SWAN
3 $\alpha$ - $\delta$	AlH	8 $\alpha$	NH
3 $\epsilon$	SiH	9 $\alpha$	OH
4 $\gamma$	CaOH		

TABLE IV °

## LINE BLEND DEPRESSIONS IN MAGNITUDES

Stars (G and K Dwarfs)

Figure Code	Color MICRONS	$\beta$ Com GOV	Sun* G2V	$\tau$ Cet G8V	$\epsilon$ Eri K2V	61 Cyg K5V	61 Cyg B K7V	Groom. 1618 MOV
$6\alpha + 8\alpha_0$	[0.336] - [0.340]	0.13	0.15	0.35	0.50	0.34	0.30	---
$6b,d + 9\alpha_{-1} + 1\alpha_b$	[0.344] - [0.354]	0.20	0.28	0.36	0.50	0.50	0.60	0.7?
$1c,d + 6\beta_1$	[0.358] - [0.368]	0.30	0.40	0.38	0.50	0.72	0.50	0.4
$1f + 2f$	[0.374] - [0.368]	0.14	0.29	0.29	0.57	0.70	0.50	0.4
$4a,b + 9\alpha_{-2}$	[0.393] - [0.402]	0.70	1.00	0.75	0.85	1.05	0.80	0.79
$5a + 6\beta_{-1}$	[0.423] - [0.426]	0.01	0.1	0.01	0.03	0.10	0.28	0.25
G	[0.430] - [0.436]	0.22	0.40	0.29	0.43	0.50	0.50	0.54
$1k + 3\alpha_0$	[0.439] - [0.436]	0.00	0.20	0.03	0.08	0.08	0.05	0.10
$1\alpha_2 + 2\alpha_1$	[0.479] - [0.472]	-0.03	0.10	-0.03	-0.07	0.10	0.08	0.17
$2\alpha_0 + 3b$	[0.518] - [0.524]	0.09	0.08	0.19	0.30	0.46	0.49	0.50
$D + 1\alpha_{-2}$	[0.589] - [0.582]	0.06	0.06	0.06	0.08	0.28	0.33	0.45
$6\alpha_B + 4\beta_0 + 1\gamma_1'$	[0.602] - [0.608]	0.02	0.00	0.02	0.03	0.05	0.05	0.02
$1\gamma_0$	[0.618] - [0.613]	-0.01	0.00	-0.02	-0.02	-0.02	0.03	0.03
$2\gamma_0$	[0.638] - [0.634]	-0.01	0.00	-0.02	0.00	-0.01	0.01	0.03

\*Solar scans by Labs and Neckel are at 20-Å resolution and narrow features show deeper depressions than our scans.



TABLE IV (continued)

Stars (M dwarfs and giants)

Figure Code	Color MICRONS	La 21185 M2V	15° 2620 M2V	4° 3561 M5V	$\alpha$ Cet M1.5III	$\delta$ Vir M3III	$\omega$ Vir M5III	$\alpha$ Her A M5Ib-II
6a + 8 $\alpha_0$	[0.336] - [0.340]	---	---	---	0.2?	0.06	-0.1	-0.1
6b,d + 9 $\alpha_{-1}$ + 1a,b	[0.344] - [0.354]	1.1	---	---	0.40	0.51	0.55	0.45
1c,d + 6 $\beta_1$	[0.356] - [0.366]	0.3	---	---	0.68	0.69	0.7	0.8
1f + 2f	[0.374] - [0.368]	0.3	---	---	0.40	0.37	0.27	0.25
4a,b + 9 $\alpha_{-2}$	[0.393] - [0.402]	0.77	1.0	---	1.29	1.25	1.15	1.34
5a + 6 $\beta_{-1}$	[0.423] - [0.426]	0.5	0.3	---	0.25	0.31	0.30	0.35
G	[0.430] - [0.436]	0.27	0.33	---	0.54	0.43	0.35	0.32
1k + 3 $\alpha_0$	[0.439] - [0.436]	0.0	0.01	---	0.07	0.06	0.00	0.03
1 $\alpha_2$ + 2 $\alpha_1$	[0.479] - [0.472]	0.16	0.25	0.2	0.05	0.15	0.28	0.22
1 $\alpha_1$	[0.497] - [0.494]	0.16	0.19	0.25	0.16	0.37	0.66	1.05
2 $\alpha_0$ + 3b	[0.518] - [0.524]	0.45	0.54	0.65	0.31	0.46	0.46	0.49
D + 1 $\alpha_{-2}$	[0.589] - [0.582]	0.57	0.57	0.95	0.26	0.43	0.53	0.56
6 $\alpha_5$ + 4 $\beta_0$ + 1 $\gamma_1'$	[0.602] - [0.608]	0.1	0.13	0.22	0.14	0.21	0.25	0.25
1 $\gamma_0'$	[0.620] - [0.613]	0.42	0.45	0.90	0.30	0.55	0.70	0.68
2 $\gamma_0$	[0.638] - [0.634]	0.08	0.07	0.10	-0.08	-0.12	-0.19	0.15

TABLE IV (continued)

Stars (G and K giants)

Figure Code	Color MICRONS	31 Com G0III	$\epsilon$ Vir G8IIIab	$\alpha$ UMa KO <sup>+</sup> IIIa	$\alpha$ Boo K2IIIp	$\alpha$ Hya K3II-III	$\alpha$ Tau K5III
6a + 8 $\alpha_0$	[0.336] - [0.340]	0.1	0.15	0.21	0.17	0.1	0.2
6b,d + 9 $\alpha_{-1}$ + 1a,b	[0.344] - [0.354]	0.2	0.12	0.21	0.30	0.30	0.32
1c,d + 6 $\beta_1$	[0.358] - [0.368]	0.30	0.68	0.74	0.75	0.80	0.74
1f + 2f	[0.374] - [0.368]	0.17	0.28	0.35	0.44	0.55	0.58
4a,b + 9 $\alpha_{-2}$	[0.393] - [0.400]	0.69	0.94	0.99	0.28	1.30	1.35
5 $\alpha$ + 6 $\beta_{-1}$	[0.423] - [0.426]	0.02	0.03	0.06	0.07	0.21	0.25
G	[0.430] - [0.436]	0.23	0.32	0.38	0.43	0.52	0.55
1k + 3 $\alpha_0$	[0.439] - [0.436]	0.03	0.05	0.06	0.05	0.06	0.1
1 $\alpha_2$ + 2 $\alpha_1$	[0.479] - [0.472]	-0.05	-0.1	-0.1	-0.07	-0.1	0.06
1 $\alpha_1$	[0.497] - [0.494]	0.00	0.00	0.00	0.00	-0.01	0.06
2 $\alpha_0$ + 3b	[0.518] - [0.524]	0.07	0.11	0.14	0.20	0.26	0.30
D + 1 $\alpha_{-2}$	[0.589] - [0.582]	0.06	0.06	0.1	0.04	0.1	0.21
6 $\alpha_5$ + 4 $\beta_0$ + 1 $\gamma_1$	[0.602] - [0.608]	0.02	0.03	0.04	0.03	0.07	0.1
1 $\gamma_0$	[0.618] - [0.613]	-0.01	-0.04	-0.03	0.02	-0.05	0.13
2 $\gamma_0$	[0.638] - [0.634]	-0.03	-0.04	-0.03	-0.03	-0.04	0.06

TABLE IV (continued)

## Stars (supergiants)

Figure Code	Color MICRONS	$\epsilon$ Gem G8Ib	$\zeta$ Aur A K4Ib	$\sigma$ CMa K7Ib	$\alpha$ Sco M1.5Iab	$\alpha$ Ori M1-M2 Ia-Ib	$\mu$ Cep M2Ia
6a + 8 $\alpha_0$	[0.386] - [0.340]	0.3	0.0	---	---	---	---
6b,d + 9 $\alpha_{-1}$ + 1a,b	[0.344] - [0.354]	0.1	0.0	---	---	0.1	---
1c,d + 6 $\beta_1$	[0.358] - [0.368]	0.70	0.85	---	0.43	0.50	---
1f + 2f	[0.374] - [0.368]	0.27	0.45	---	0.05	0.18	---
4a,b + 9 $\alpha_{-2}$	[0.393] - [0.402]	1.15	1.25	1.27	0.7	1.17	1.3
5a + 6 $\beta_{-1}$	[0.423] - [0.426]	0.09	0.2	0.29	0.21	0.21	0.3
G	[0.430] - [0.436]	0.41	0.56	0.63	0.49	0.55	0.66
1k + 3 $\alpha_0$	[0.438] - [0.432]	0.09	0.08	0.09	0.07	0.09	0.07
1 $\alpha_2$ + 2 $\alpha_1$	[0.479] - [0.472]	-0.17	-0.09	-0.05	-0.06	-0.03	-0.07
1 $\alpha_1$	[0.497] - [0.494]	-0.02	-0.04	0.07	0.14	0.16	0.19
2 $\alpha_0$ + 3b	[0.518] - [0.524]	0.12	0.31	0.31	0.25	0.27	0.31
D + 1a $_{-2}$	[0.589] - [0.582]	0.06	0.06	0.27	0.26	0.33	0.33
6 $\alpha_6$ + 4 $\beta_0$ + 1 $\gamma_1^i$	[0.602] - [0.608]	0.04	0.08	0.12	0.16	0.16	0.18
1 $\gamma_0^i$	[0.618] - [0.613]	0.00	0.02	0.12	0.22	0.28	0.26
2 $\gamma_0$	[0.638] - [0.634]	-0.05	-0.05	-0.12	-0.13	-0.13	-0.10

ÅNGSTROMS

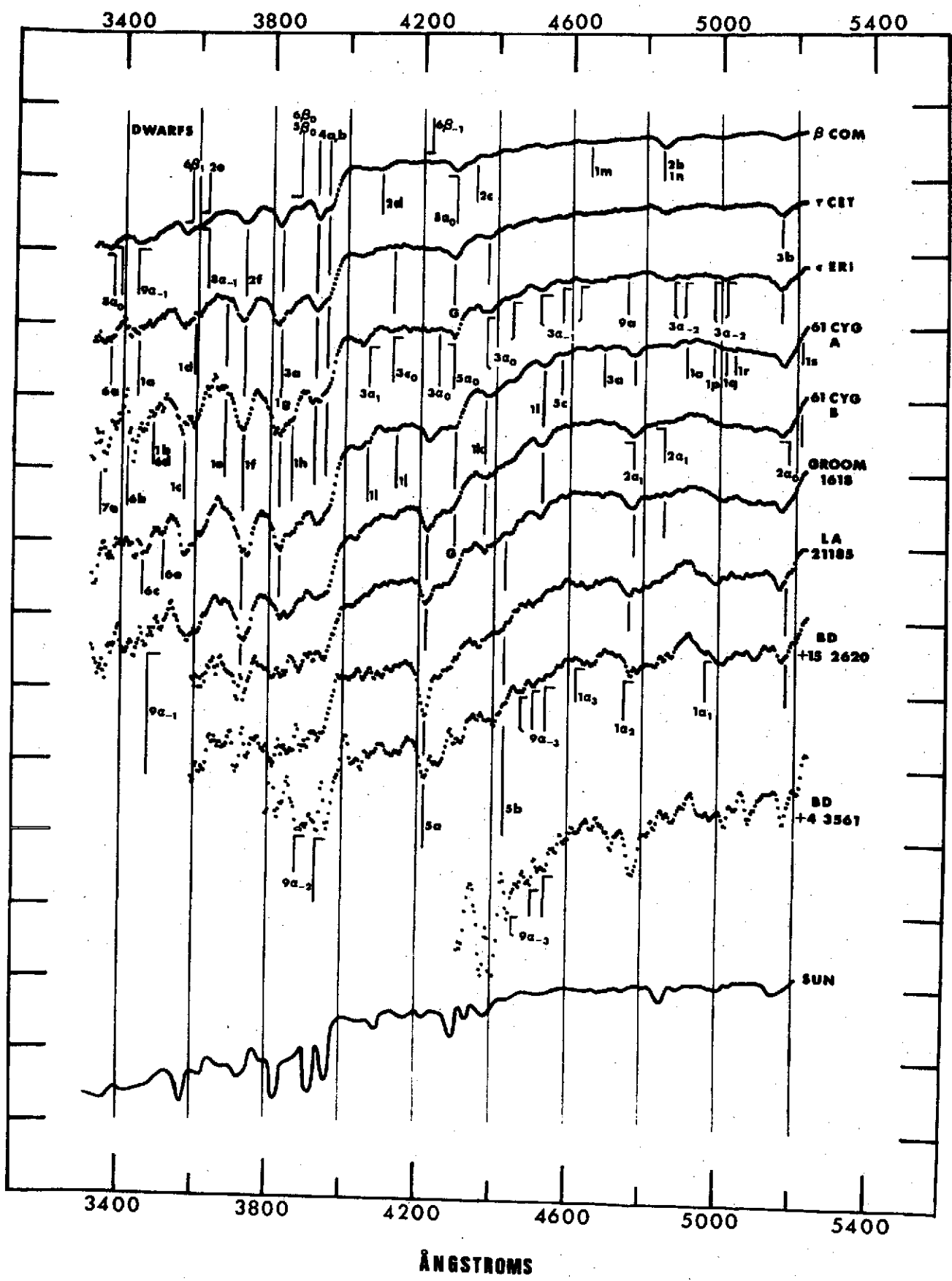


Fig 1

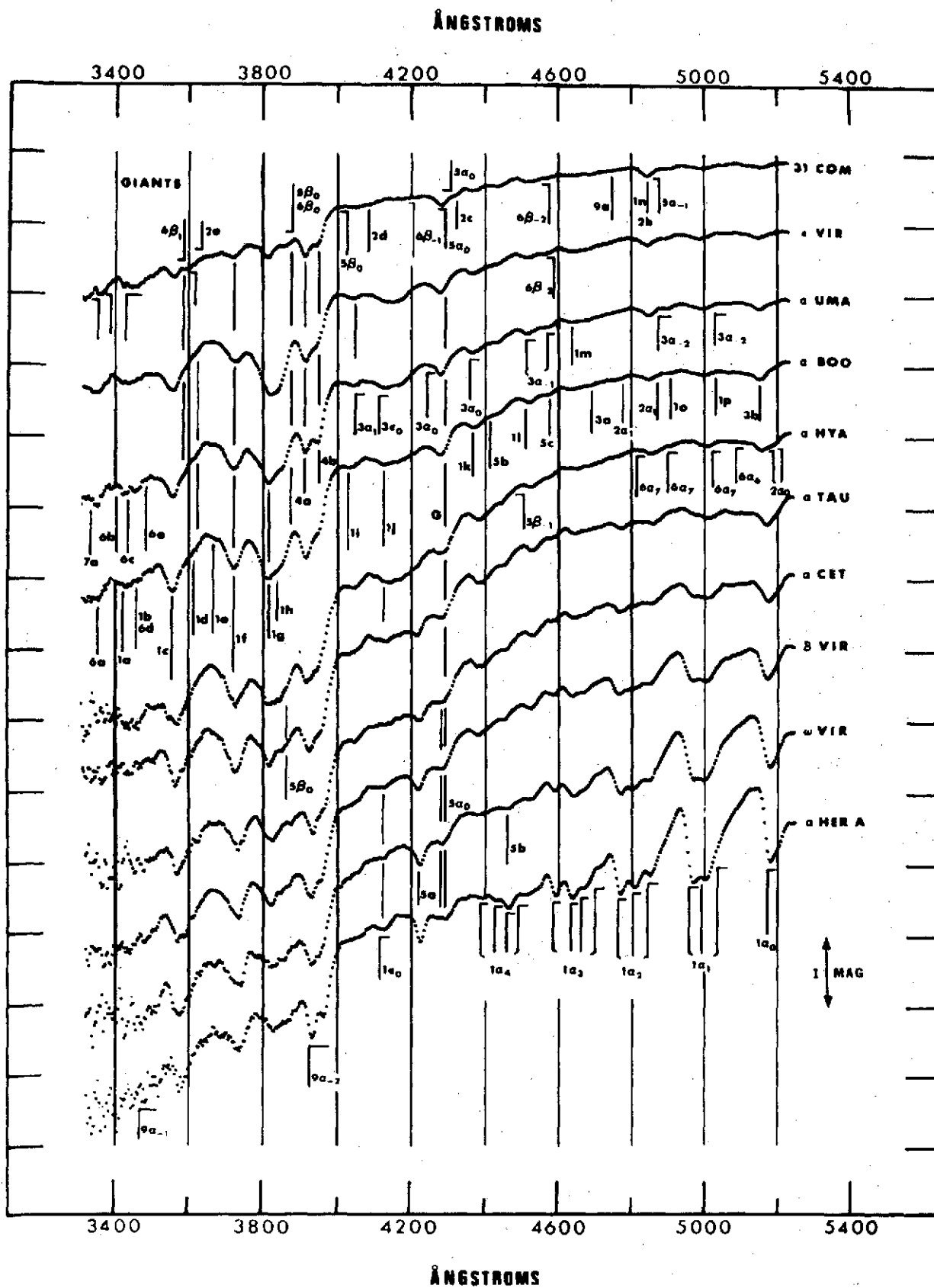
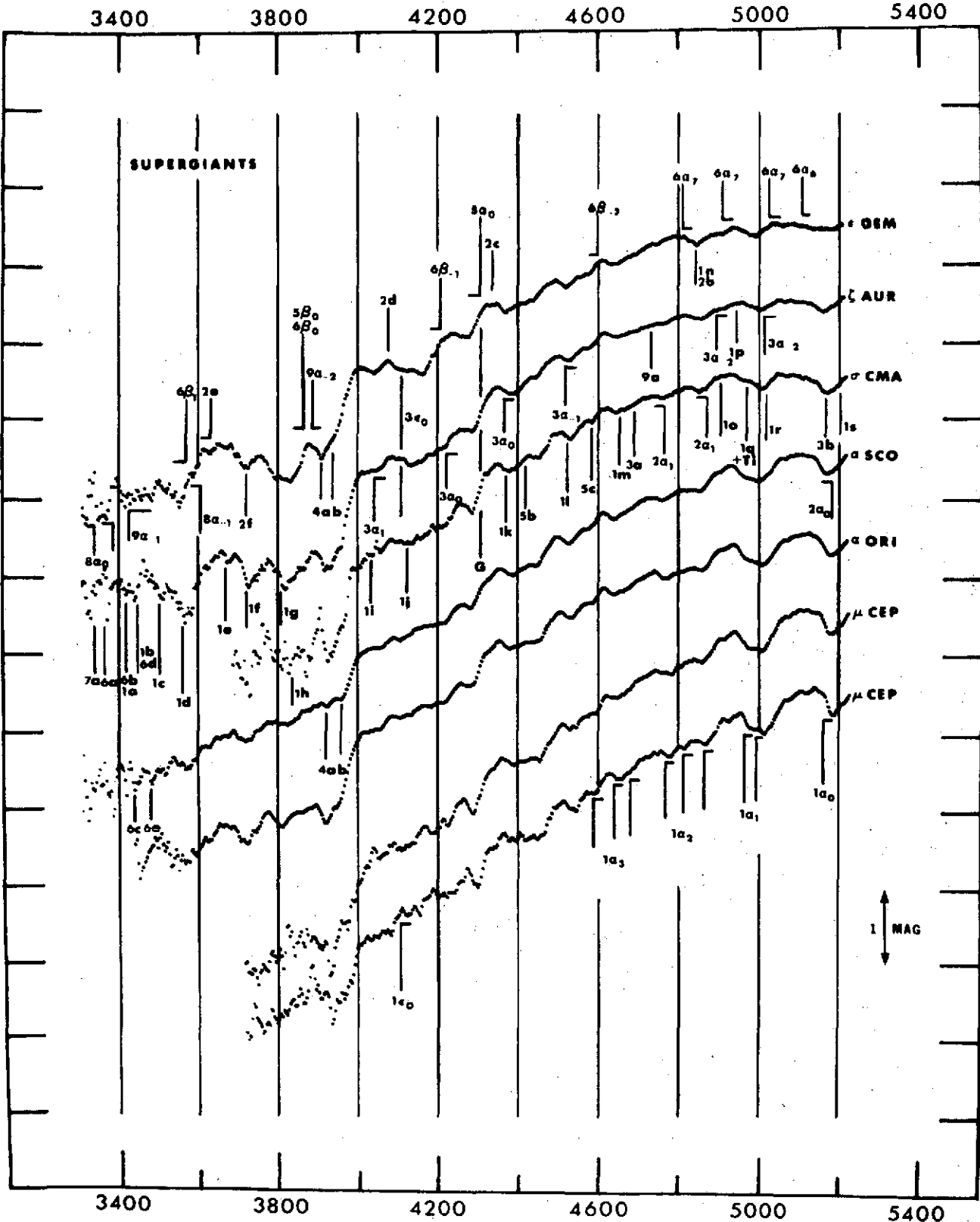


Fig 2

ÅNGSTROMS



ÅNGSTROMS

Fig 3

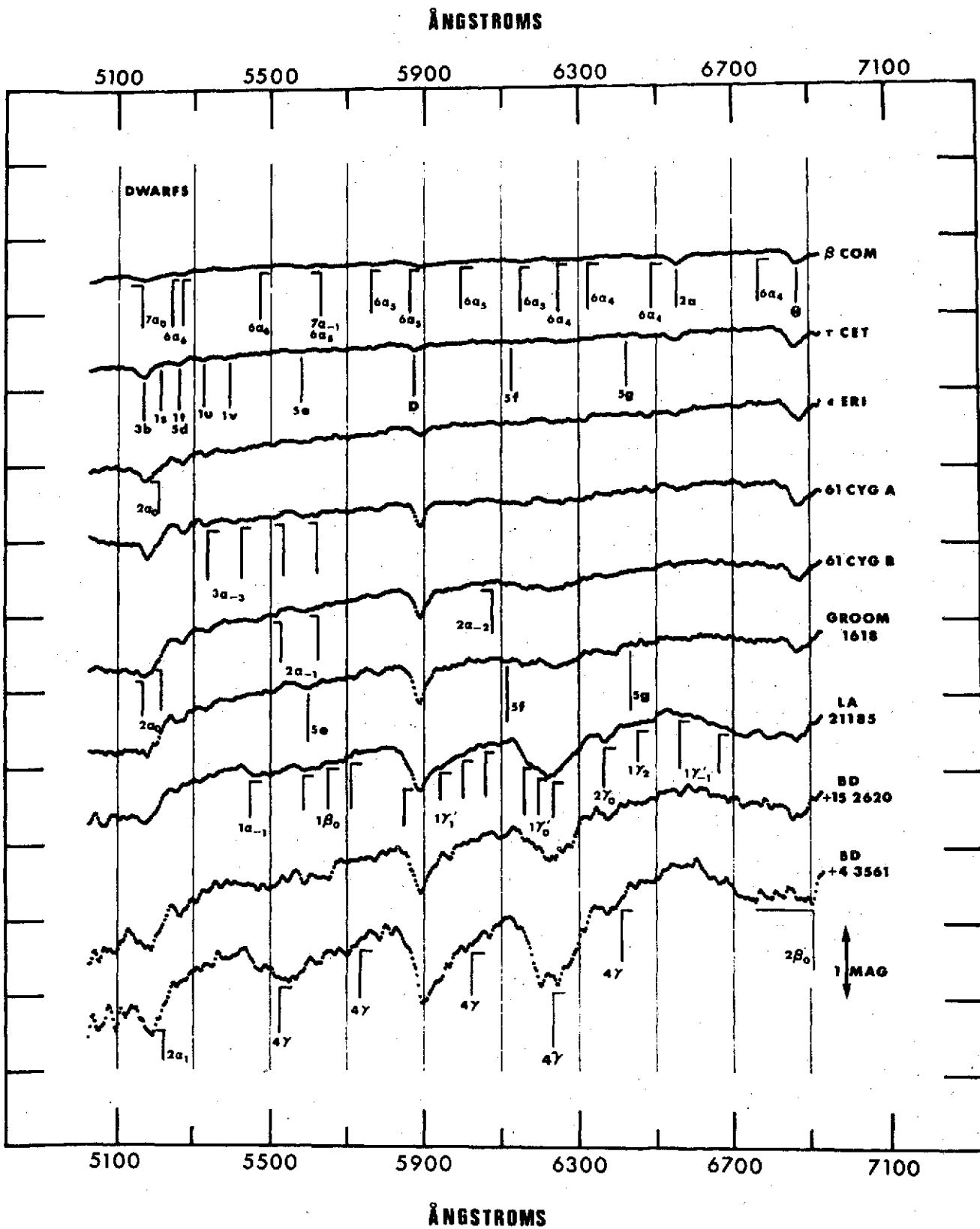


Fig 4

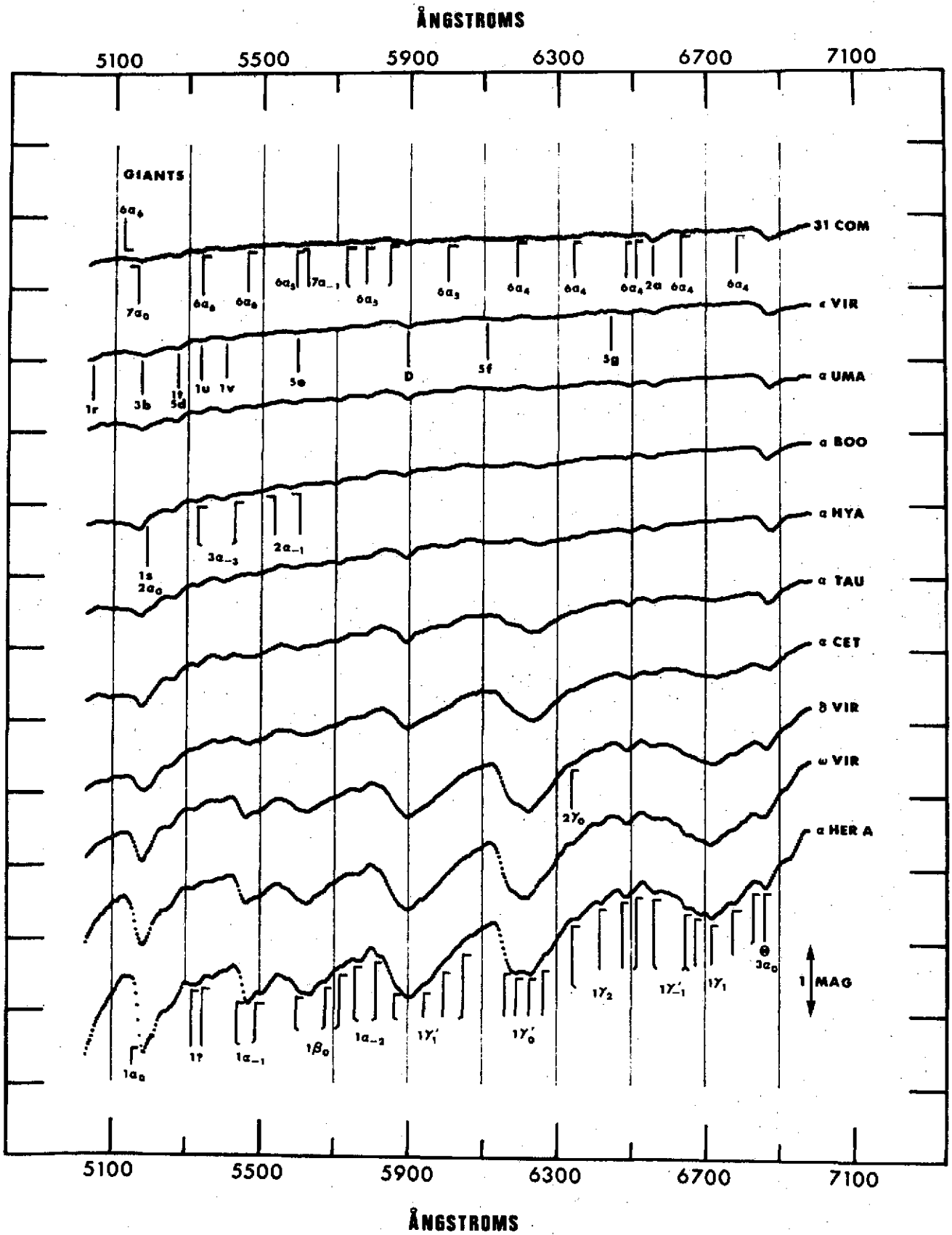


Fig 5



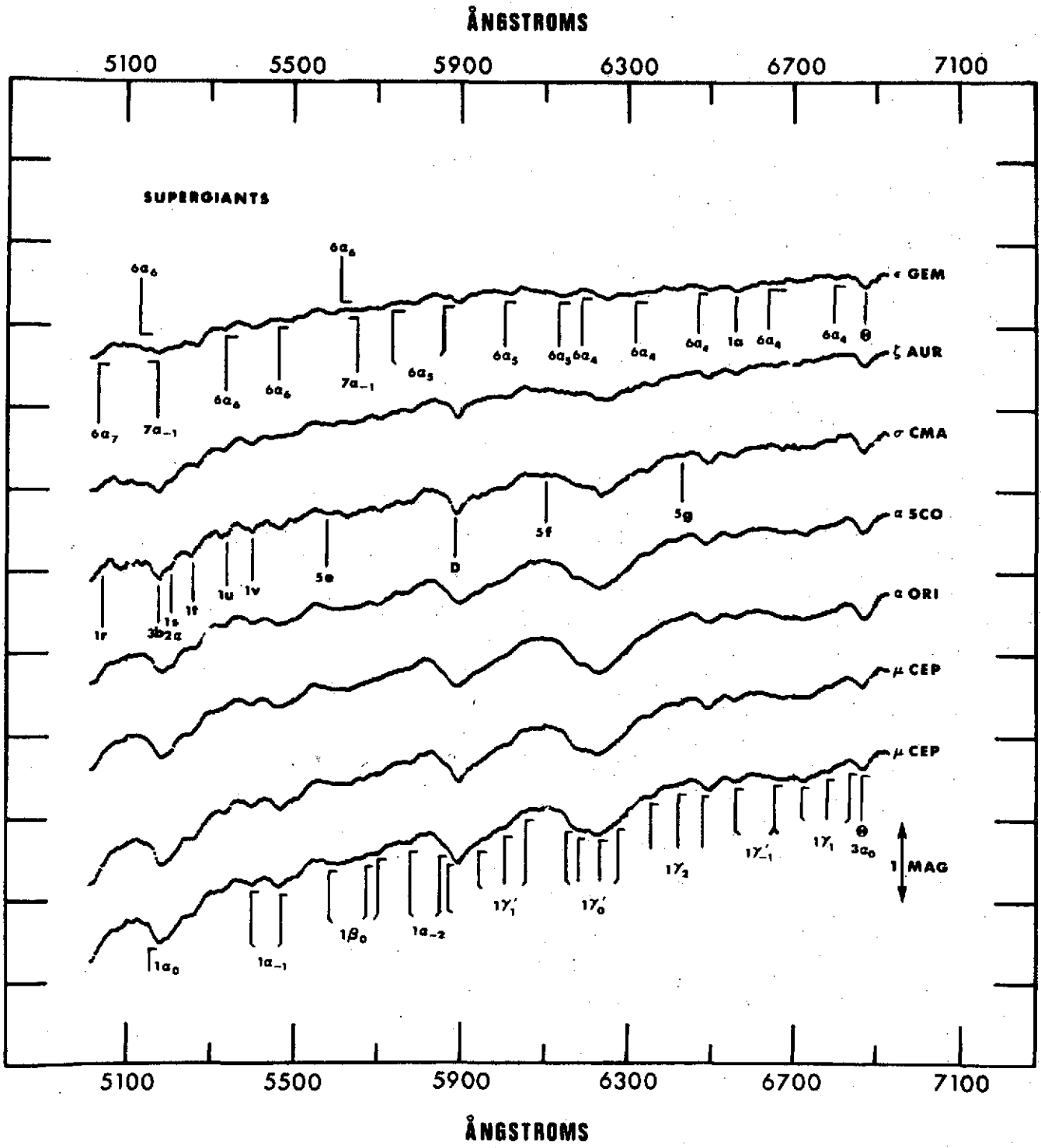


Fig. 1

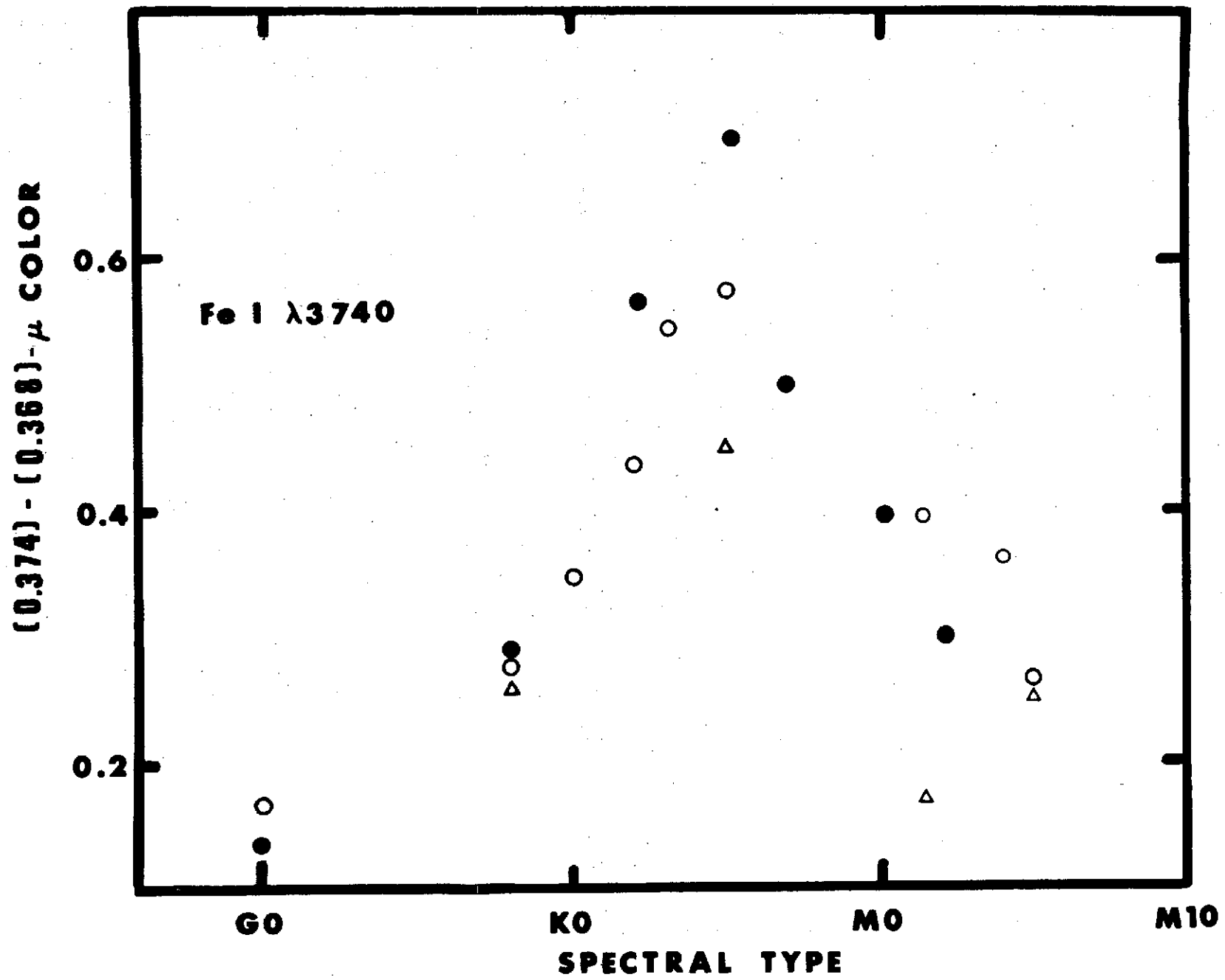


Fig 7

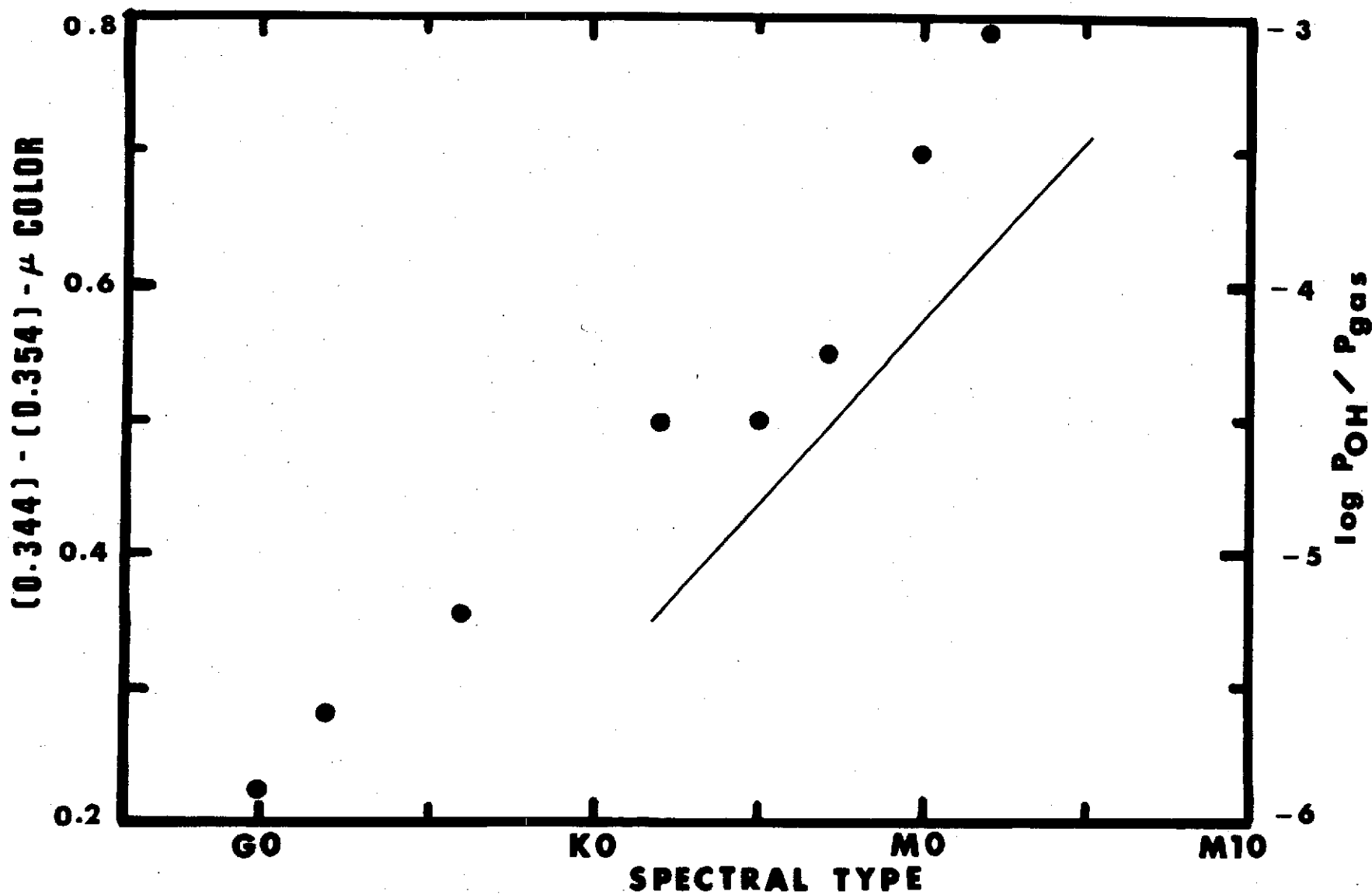


Fig 8